Charge-transfer induced by Pb-doping and annealing in Bi-2212 phase superconductor

2001 J. Phys.: Condens. Matter 13 5195

(http://iopscience.iop.org/0953-8984/13/22/313)

INSTITUTE OF PHYSICS PUBLISHING JOURNAL OF PHYSICS: CONDENSED MATTER

J. Phys.: Condens. Matter **13** (2001) 5195–5204 www.iop.org/Journals/cm PII: S0953-8984(01)20162-3

Charge-transfer induced by Pb-doping and annealing in Bi-2212 phase superconductor

Lei Shi, Chen Li, Qiuzhao Dong and Yuheng Zhang

Structure Research Laboratory, University of Science and Technology of China, Academia Sinica, Hefei, Anhui 230026, People's Republic of China

Received 15 December 2000, in final form 6 April 2001

Abstract

A systematic study of Pb-doping and annealing effects in vacuum (2×10^{-3} Pa) on T_c and the microstructure of $Bi_{2-x}Pb_xSr_2CaCu_2O_\delta$ compounds has been carried out. It is found that the structure belongs to the Bi-2212 phase. The *c*- and *b*-axes almost keep unchanged while Bi is replaced by Pb. With increasing annealing temperature, *c*- and *b*-axis parameters monotonically increase while the *a*-axis parameter is unchanged. The modulated period becomes longer and finally disappears with increasing Pb content and annealing temperature. Meanwhile, the distortion of CuO_2 planes becomes serious. There is an optimum T_c with increasing annealing temperature, which reveals that the carrier concentration p changes from overdoped to underdoped. It is suggested that the differences of both the valences and the ionic sizes of Pb^{2+} and Bi^{3+} cause the reduction of extra oxygen, resulting in the increasing positive charge in the BiO double planes. The distortion of CuO_2 planes is partially caused by the increase of positive charge in BiO double planes. A charge-transfer between the carrier reservoir (BiO–SrO) and the conducting CuO_2 plane is induced by Pb-doping and annealing in vacuum. Both the distortion of CuO_2 planes and the charge-transfer control the carrier concentration and carrier distribution in CuO_2 planes, which is related to the superconductivity of the Pb-doped Bi-2212 phase.

1. Introduction

The high-T_c cuprate superconductors constitute a special group of materials that share many common features in crystal structure and properties. One of the characteristic structural features is that they have layered crystal structures with the two-dimensional (2D) CuO_2 layers, which are the most essential structural elements for high-T_c superconductivity, and charge reservoirs [1] like $Bi_2O_{2+\delta}$ that are necessary to provide charge carriers for superconductivity. Like other high-T_c cuprates, the Bi compounds have layered crystal structures with alternating rock-salt blocks and perovskite blocks which form a homologous system $Bi_2Sr_2Ca_{n-1}Cu_nO_{2n+4+\delta}$ with $T_c^{max} = 20$, 85 and 110 K for $n = 1$, 2 and 3 [2], respectively. In fact, a single phase $n = 3$ Bi compound has not been grown without cation (such as Pb) doping. In contrast

0953-8984/01/225195+10$30.00

with Bi compounds, however, single phase samples with similar $n = 1$, 2 or 3 structures to Bi compounds for the $Tl_2Ba_2Ca_{n-1}Cu_nO_{2n+4+\delta}$ series can be easily made without cation doping [3, 4]. The T_c^{max} of the Tl compound is 90, 115 and 125 K for $n = 1$, 2 and 3 [5], respectively. Corresponding to the same n, the T_c^{max} of Bi compounds and Tl compounds is rather different. The T_c^{max} difference is, for example, 25 and 10 K for $n = 2$, 3, respectively. It is worth noting that both Bi compounds and Tl compounds have a similar crystal structure, or average atomic structure. Tl and Bi have the same valence and nearly the same ionic sizes. Their micro-structures are, however, different: Bi-based superconductors occupy intense incommensurate modulated structures, but Tl-based superconductors do not. These structural modulations for the Tl family are due to only small deviations of the atoms from their mean positions [6], but for the Bi members the positional distortions are large. It seems that the differences in the micro-structures may bring about different electronic characteristics among them.

Pham *et al* [7] have studied in detail the variation of T_c and the structural modulation with annealing conditions of $Bi_2Sr_2CaCu_2O_8$, $Bi_{2.1}Sr_{1.9}CaCu_2O_{8+\delta}$ and an air-prepared 2212 mixture. It is found that for stoichiometric $Bi_2Sr_2CaCu_2O_8$ the maximum of T_c corresponds to an oxygen content close to 8 and treatments in air produce only a slight increase of the oxygen content, decreasing the T_c a few degrees but reducing significantly the modulation period (4.91 to 4.7). For the other samples the T_c goes through a maximum ($\approx$90 K) and then decreases with increasing oxygen content. Calestani *et al* [8] have investigated the $(Bi, Pb)_2Sr_2(Ca, Y)Cu_2O_z$ system and pointed out the existence of a modulation-free 2212 phase over a wide range of composition ($Bi_{2-x}Pb_xSr_2Y_{1-y}Ca_yCu_2O_z$, $0 \leqslant y \leqslant 0.8$ and $x = (1 - y/2) \pm 0.2$). The non-modulated $Bi_{2-x}Pb_xSr_2Y_{1-y}Ca_yCu_2O_z$ phase still shows superconductivity in the Ca-rich region with T_c decreasing with increasing Y content, supplying a further example of superconductivity not being related to the structural modulation in the Bi system.

To understand the layered copper oxide superconductors, a local charge picture has been proposed by Cava [1]. At the centre of the local charge picture is the idea that all the layered copper oxide superconductors have crystal structures that can be considered as built of electronically active CuO_x superconducting layers sandwiched between other structural layers which act as spacers, and, most importantly, as electronic charge reservoirs. The doping of the active CuO_x layers is controlled by the electronic state of the charge reservoirs. Each of the kinds of charge reservoir layer presently known has its own characteristic behaviour in transferring charge to or from the CuO_x planes. High-T_c superconductivity is created by doping (adding charge carriers to) a 'Mott' insulator [9]. Although the structural relationships in the layered copper oxide superconductors can be clarified, the means by which the charge reservoir layers act electronically on the CuO_2 double planes is by no means straightforward. The connection of charge transfer and the micro-structure is still unclear.

Aliovalent cation substitutions can change the effective copper valence and the carrier concentration, which is intimately linked with T_c. Therefore, aliovalent cation substitution in cuprate has been one of the basic methods to investigate the mechanisms of high-T_c superconductors. By substitution of rare-earth elements for Ca in $Bi_2Sr_2CaCu_2O_y$, a transition from superconductor to insulator is found to occur with progressive substitution of rare earths, and this transition has been attributed to a decrease in the carrier concentration. Groen *et al* [10] found that rare-earth ion doping in the Sr site of $Bi_2Sr_2CuO_\delta$ is accompanied by incorporation of extra oxygens, and enhancement of T_c up to 30 K. By substitution of Pb for Bi in $Bi_2Sr_2CaCu_2O_y$, in this paper, the microstructure is changed by Pb dopant and the extra oxygen located in Bi_2O_2 layers is decreased by annealing in vacuum with different temperature and time. The relationship of microstructure and T_c is studied.

2. Experimental methods

The samples of $Bi_{2-x}Pb_xSr_2CaCu_2O_\delta$ ($x = 0$–0.5) were prepared by a conventional solid state reaction method starting from high-purity powder of Bi_2O_3, PbO, $SrCO_3$, CuO and $CaCO_3$ in the appropriate ratios required for an overall 2212 stoichiometry. The intimate mixtures were sintered in air at 780 °C for 24 h, then reground and sintered in air at 810 °C for 24 h. Finally, the resulting powder was reground and pressed into pellets and calcinated between 820 and 840 °C for 24 h and furnace-cooled in air. All the samples were annealed in vacuum (of degree 2×10^{-3} Pa) at a temperature of 500 °C for 2 hours. The $x = 0.4$ sample was annealed in vacuum at annealing temperature 350 °C, 400 °C, 500 °C, 550 °C, 600 °C, 650 °C, respectively, for 3.5 hours, or at 500 °C for different times, respectively. The absolute oxygen content of the samples was determined by iodometric titration.

X-ray diffraction (XRD) analysis was carried out by a Mac Science M18X diffractometer with graphite monochromatized Cu Kα ($\lambda = 1.540\,18$ Å) radiation. The lattice parameters of some selected samples were obtained by a least-squares fit of peak positions. The resistivity dependence on temperature was measured by using a standard four-probe method in a closed-cycle helium cryostat C50W. The temperature range for the measurement was from 14 to 300 K. The electron diffraction patterns were performed by using a transmission electronic microscope (TEM), type H-800. Raman spectra of the samples were performed on a Spex-1403 Raman spectrophotometer by using a back-scattering technique. The 5145 Å line from an argon ion laser was used as an excitation light source.

3. Experimental results

3.1. XRD and ED analysis of the $Bi_{2-x}Pb_xSr_2CaCu_2O_\delta$ ($x = 0$–0.5) samples

The XRD patterns show that all the samples belong to the Bi-2212 phase. No impurity can be detected. For the unannealed $Bi_{2-x}Pb_xSr_2CaCu_2O_\delta$ ($x = 0$–0.5) samples, the XRD patterns give a tetragonal symmetry. The *a*- and *c*-axes of the unannealed samples have little change with increasing Pb content x (figure 1(a)). To control the oxygen content, the $Bi_{1.6}Pb_{0.4}Sr_2CaCu_2O_\delta$ samples were annealed in vacuum. It is found that the structure is changed gradually from tetragonal to orthorhombic with increasing annealing temperature. As the annealing temperature rises from 350 to 650 °C (figure 1(b)), the *c*-axis and *b*-axis parameters monotonically increase while the *a*-axis parameter is unchanged. The changing of oxygen content of $Bi_{1.6}Pb_{0.4}Sr_2CaCu_2O_\delta$ dependent on annealing temperature is shown in figure 2. From figure 2 it is found that the oxygen content monotonically decreases while the annealing temperature increases, which is consistent with the changing of the *c*- and *b*-axes in figure 1(b). These results reveal that the extra oxygen in Bi_2O_2 layers is removed by annealing.

Figure 3 shows the electron diffraction (ED) patterns of some selected samples. These patterns are measured in the *ab*- (001) plane in which the change of the modulated period is observed. It is well known that there is an incommensurate modulated structure along the *b*-axis in the Bi2212 superconductor. The incommensurate modulated structure is thought to be due to an excess of oxygen atoms inserted in the Bi–O layers, or to the intrinsic property of the Bi^{3+} $6s^2$ lone pair [11]. Figure 3(a) exhibits that with increasing Pb content, the modulated structure gradually weakens; that is, the modulated wavelength increases. The ratio of the modulated wavelength of $Bi_{2-x}Pb_xSr_2CaCu_2O_\delta$ ($x = 0$–0.5) to the *b*-axis is 4.69, 4.84, 5.21, 5.36, 7.50, 10.71, respectively. Observed from figure 3(b), it is found that the modulated wavelength of the annealed $Bi_{1.6}Pb_{0.4}Sr_2CaCu_2O_\delta$ sample further increases with rising annealing temperature.

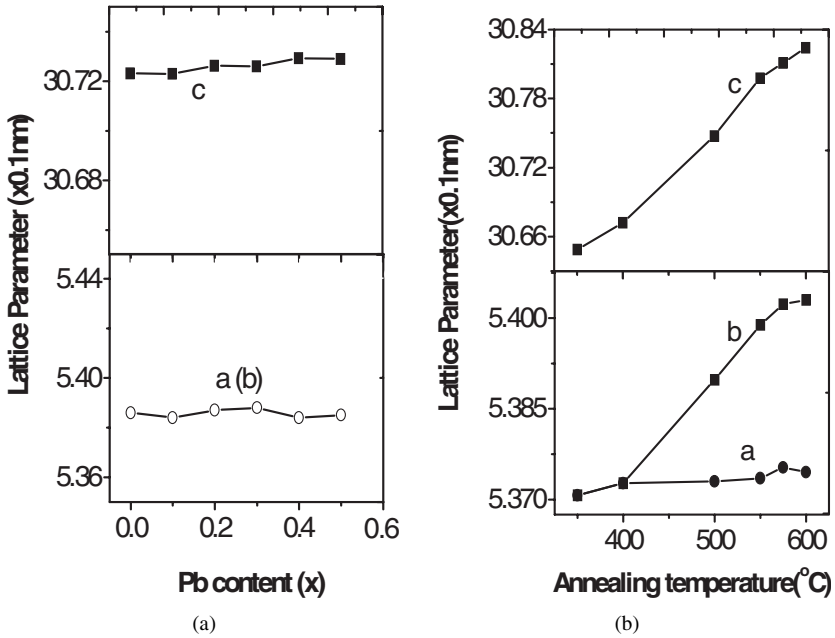

Figure 1. Lattice parameter for (a) unannealed $Bi_{2-x}Pb_xSr_2CaCu_2O_\delta$ ($x = 0$–0.5) samples against the dopant content and (b) $Bi_{1.6}Pb_{0.4}Sr_2CaCu_2O_\delta$ annealed at different temperature for 3.5 hours against different annealing temperature.

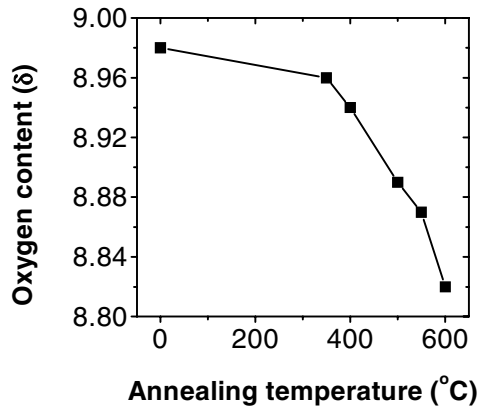

Figure 2. Oxygen content δ change of $Bi_{1.6}Pb_{0.4}Sr_2CaCu_2O_\delta$ dependent on annealing temperature.

The ratio of the modulated wavelength of the annealed $Bi_{1.6}Pb_{0.4}Sr_2CaCu_2O_\delta$ sample to the *b*-axis increases from 7.90 to 9.38 to 12.50 with annealing temperature rising from 350 to 500 to 650 °C. Both Bi replaced by Pb and annealing in vacuum lead to oxygen content decreasing, thus causing the modulated wavelength become longer.

The lengths of *a*- and *b*-axes are considered to be controlled by the in-plane Cu–O bond distance, which is closely related to the carrier concentration [12]. The *a*- and *b*-axis parameters should be decreased due to the hole concentration increase, which can strengthen the Cu–O bonding force when Pb content increases [12]. Similarly to the *c*-axis, the parameter change can

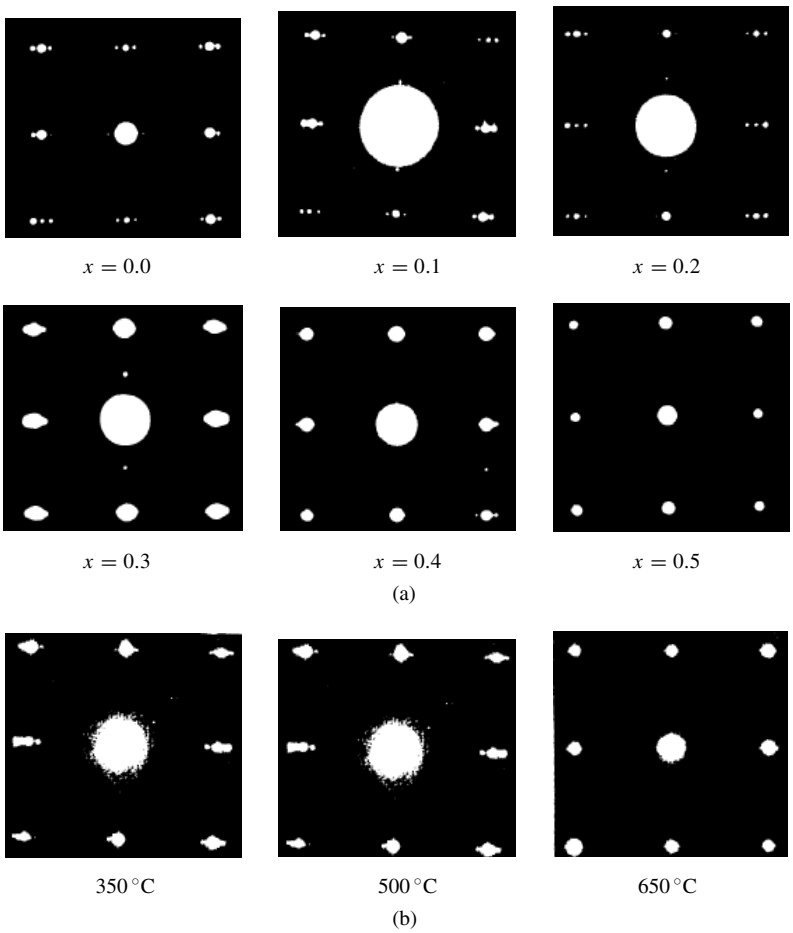

Figure 3. Electron diffraction patterns for (a) unannealed $Bi_{2-x}Pb_xSr_2CaCu_2O_\delta$ ($x = 0$, 0.1, 0.2, 0.3, 0.4, 0.5) and (b) $Bi_{1.6}Pb_{0.4}Sr_2CaCu_2O_\delta$ annealed at 350, 500 and 650 °C for 3.5 hours.

arise from the variance of extra oxygen induced by the aliovalent substitution. But figure 1(a) shows that as the Pb content increases from $x = 0$ to 0.5, the lattice parameters have no obvious change. This means that the effect of Pb doping on the microstructure of the Cu–O plane in Pb-substituted Bi2212 is small. The unchanged lattice parameter can be explained by both the change of excess oxygen content and the ionic size difference of Pb^{2+} and Bi^{3+}. The ionic size of Pb^{2+} ($R = 0.12$ nm) is considerably larger than that of Bi^{3+} ($R = 0.093$ nm). Thus, by considering the ionic size alone, the substitution of Pb increases the lattice parameters. On the other hand, after doping Pb in the Bi site, the valence of Cu and Bi is unchanged, which are +2 and +3 respectively, only the average valence of (Bi–Pb) decreases [13]. The difference in the valences between Pb^{2+} and Bi^{3+} lowers the extra oxygen content and decreases the lattice parameters. The opposite reaction of ionic size and ionic valence on lattice makes the substitution of Pb for Bi have little effect on the structure of the samples so that the average structures have no distinct change. However, the reduction of extra oxygen incorporated in Bi_2O_2 layers caused by the substitution of Pb definitively affects the modulation structure, as shown in ED patterns. The Pb-doped Bi-2212 superconductors are still in an overdoped state [14].

Nagoshi *et al* [15] have reported that both the *c*- and *b*-axis of the undoped Bi-2212 superconductor increase as the oxygen content decreases, which was caused by annealing in vacuum. Owing to the excess oxygen decreasing, the incommensurate modulation weakens so that the degree of the mismatch between the Bi_2O_2 and the perovskite layer is weakened [16]. The stress of the perovskite layer is released, thus leading to the elongation of the *b*-axis. Similarly after annealing, the hole concentration decreases. The elongation of the *b*-axis, which is controlled by the in-plane Cu–O bond distance, can be interpreted by the weakening Cu–O bonding caused by the decreasing hole concentration [12]. For *c*-axis elongation induced by the change of excess oxygen, one explanation [17] is that the decrease of extra oxygen incorporated into Bi_2O_2 layers leads to a change of the orientation of the Bi^{3+} lone pair, which causes an increase of the distance of the two adjacent BiO layers.

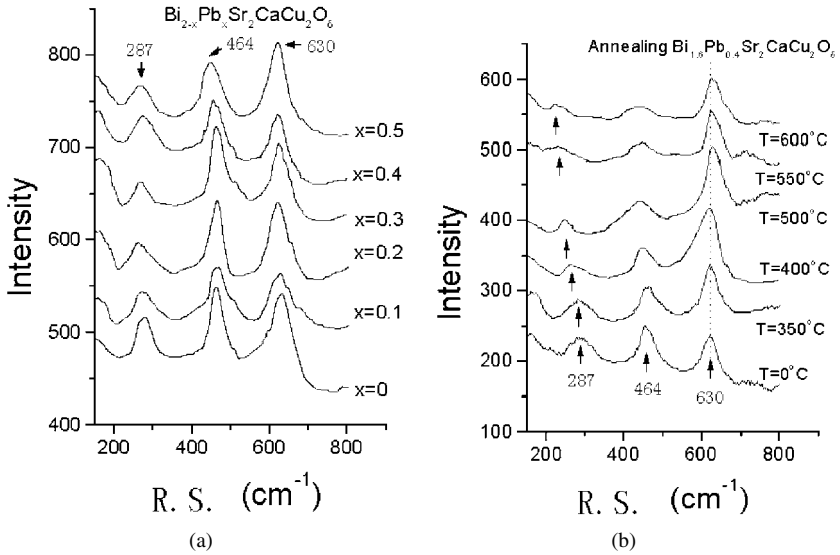

Figure 4. Raman spectrum patterns for (a) unannealed $Bi_{2-x}Pb_xSr_2CaCu_2O_\delta$ ($x = 0$–0.5) samples; (b) $Bi_{1.6}Pb_{0.4}Sr_2CaCu_2O_\delta$ annealed at different temperatures for 3.5 hours. (R.S. = Raman shift.)

3.2. Raman scattering analysis of the $Bi_{2-x}Pb_xSr_2CaCu_2O_\delta$ ($x = 0$–0.5) samples

Clearly the structural change mentioned above should be displayed in the Raman spectra. The Raman spectra of the samples are shown in figures 4(a) and (b) respectively. Three vibration modes of 287, 464, 630 cm^{-1} for $Bi_{2-x}Pb_xSr_2CaCu_2O_\delta$ ($x = 0$–0.5) and annealed $Bi_{1.6}Pb_{0.4}Sr_2CaCu_2O_\delta$ are visible in figure 4. In figure 4(a), the peaks change little with increasing Pb content, which is in accordance with the fact that the *a*-, *b*- and *c*-axis parameters keep unchanged with increasing Pb content in figure 1(a). Figure 4(b) shows the Raman peaks for annealed $Bi_{1.6}Pb_{0.4}Sr_2CaCu_2O_\delta$, in which the 630 cm^{-1} mode is almost unaffected by annealing, while the intensities of 464 and 287 cm^{-1} modes change with annealing temperature increasing. The frequency of 287 cm^{-1} slightly decreases.

The 464 cm^{-1} mode has been assigned to $O(3)_{Bi}$ A_{1g} *c*-axis vibration [18, 19] (A_{1g} nodes are symmetric *c*-axis vibration of Bi, Sr, $O(1)_{Cu}$, $O(2)_{Sr}$ and $O(3)_{Bi}$), which is connected with the more labile oxygen atoms in the Bi_2O_2 layer. In figure 4(b), it is clear that the 464 cm^{-1} peak intensity decreases with increasing annealing temperature. Annealing in vacuum causes

excess oxygen loss in the Bi_2O_2 layer. The oxygen loss directly influences the Bi_2O_2 plane and the distance of the BiO–BiO layers, with a result of the Bi–$O(3)_{Bi}$ bond increasing and the broadening and the weakening of the Raman peak while the red-shift is not apparent. The 630 cm^{-1} mode has been assigned to $O(2)_{Sr}$ A_{1g} vibration along the c-axis [18, 19]. In this experiment, for the 630 cm^{-1} mode, the frequency and intensity almost keep unchanged with increasing annealing temperature. Because the replacement of Pb for Bi takes place in the Bi_2O_2 planes, the Bi_2O_2 layer is directly influenced. This indicates that annealing in vacuum does not affect the microstructure of the SrO layer.

It is worth noting that the 287 cm^{-1} mode, which has been assigned to the B_{1g} modes, is an out-of-phase vibration of $O(1)_{Cu}$ atoms along the c-axis. It is directly related to the conducting CuO_2 planes and exhibits a pronounced asymmetry induced by a Fano interferent between the phonon and an electronic scattering background. From figure 4(b), the intensity of 287 cm^{-1} clearly decreases and the peak position shifts to low wavenumber with increasing annealing temperature. This result and the change of lattice parameters in figure 1(b) prove the distortion of the CuO_2 plane: with the elongation of the b-axis, the Cu–O(1) bond weakens, which indicates that the effect of Cu on O(1) decreases. Meanwhile the carrier concentration of the carrier reservoir increases due to a reduction of the extra oxygen atoms. This enhances the exchange interaction between the carrier reservoir and the $O(1)_{Cu}$ atom, leading to the deviation of $O(1)_{Cu}$ atom from CuO_2 plane. Therefore the Raman peak of the $O(1)_{Cu}$ atom shifts to low wavenumber. Observed from figure 1(b) and figure 4(b), with the annealing temperature rising, the longer the b-axis, the weaker the $O(1)_{Cu}$ Raman peak (red-shift) so that the distortion of the CuO_2 plane becomes bigger and bigger. The micro-structural change of the conductive CuO_2 planes should affect the superconductivity.

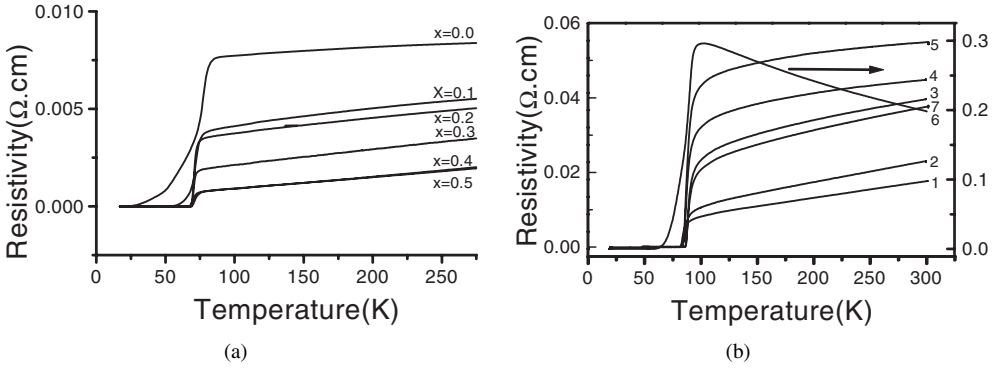

Figure 5. The temperature dependence of the resistivity for (a) unannealed $Bi_{2-x}Pb_xSr_2CaCu_2O_\delta$ (x = 0–0.5) samples; and (b) $Bi_{1.6}Pb_{0.4}Sr_2CaCu_2O_\delta$ at annealing temperature 1, T = 350 °C, 2, T = 400 °C, 3, T = 500 °C, 4, T = 550 °C, 5, T = 600 °C, 6, T = 650 °C for 3.5 hours, and 7, T = 500 °C for 2 hours.

3.3. Electronic transport properties of the $Bi_{2-x}Pb_xSr_2CaCu_2O_\delta$ (x = 0–0.5) samples

Figure 5(a) shows the temperature dependence of the resistivity for $Bi_{2-x}Pb_xSr_2CaCu_2O_\delta$ (x = 0–0.5). For the sample x = 0.0, T_c^{onset} is 84 K, T_{C0} is 25 K, $\Delta T = T_c^{onset} - T_{C0}$ is the superconducting transition width. With Pb content increasing from 0.0, 0.1, 0.2, 0.3, 0.4 to 0.5, ΔT is 59, 20.13, 6.23, 3.88, 3.46 and 2.35 K respectively. The very broad ΔT in x = 0.0 is clearly due to oxygen inhomogeneity. From both figure 3(a) and figure 5(a), it is found that with increasing Pb content, Pb doping weakens the incommensurate modulation

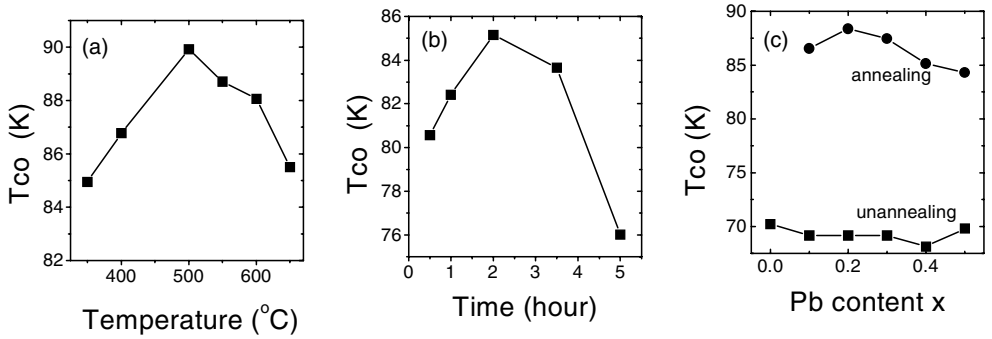

Figure 6. (a) T_{C0} of $Bi_{1.6}Pb_{0.4}Sr_2CaCu_2O_\delta$ dependence on the annealing temperature for 3.5 hours and (b) the annealing time at 500 °C; (c) T_{C0} of annealed and unannealed samples $Bi_{2-x}Pb_xSr_2CaCu_2O_\delta$ ($x = 0$–0.5).

and decreases ΔT, which stabilizes the Bi-2212 phase. Meanwhile, the Pb doping reduces the extra oxygen. This result reveals that the oxygen inhomogeneity mainly comes from the disorder distribution of extra oxygen. We also noticed that the normal-state resistivity systematically decreases with increasing Pb content, implying an increased number of charge carriers. The increase of the carrier concentration has been interpreted as a result of electron vacancy due to the additional holes contributed by the aliovalent Pb^{2+} ion replacing the trivalent Bi^{3+}. Obviously the Pb-doped samples lie in the overdoped state [19]. In order to adjust the carrier concentration, the sample with $x = 0.4$ was annealed in vacuum. Figure 5(b) shows the temperature dependence of resistivity for annealed $Bi_{1.6}Pb_{0.4}Sr_2CaCu_2O_\delta$ at different annealing temperature for 3.5 hours. It is found that the optimum T_c appears at 500 °C. Then we annealed the samples at 500 °C for different annealing time (figure 6(a)). The result reveals that the optimum annealing temperature and annealing time is 500 °C and 2 hours (figure 6(b)). Therefore in the same conditions, we annealed the other samples. Figure 6(c) reveals the temperature dependence of resistivity for $Bi_{2-x}Pb_xSr_2CaCu_2O_\delta$ ($x = 0.1$–0.5, annealing temperature: 500 °C, annealing time: 2 hours). It is obvious that after annealing, the T_{C0} greatly increases by 15 K or so for $Bi_{2-x}Pb_xSr_2CaCu_2O_\delta$ ($x = 0.1$–0.5). The optimum T_c appears in the sample $Bi_{1.6}Pb_{0.4}Sr_2CaCu_2O_\delta$ at annealing temperature 500 °C, annealing time 2 hours. Obviously the optimum superconductivity does not appear in the most distorted CuO_2 plane, but in an optimum distortion. Observed from figure 3 and figure 4, the maximum distortion of CuO_2 plane occurs at annealing temperature 650 °C for 3.5 hours. The optimum T_{C0} is 87 K at annealing temperature 500 °C, annealing time 2 hours, which shows that CuO_2 plane occupies an optimum distortion.

4. Discussion

It is well known that the Bi-2212 superconductor possesses a strong incommensurate modulation structure due to a lattice mismatch between the Bi_2O_2 layers and the perovskite-like blocks. In order to stabilize the crystal structure, extra oxygen is induced in the Bi_2O_2 layer. In this work, the ED patterns show that the substitution of Pb for Bi, as well as annealing in vacuum, decreases the superlattice modulation. The extra oxygen located in the Bi_2O_2 layers decreases with Pb content x and/or increasing annealing temperature [19].

The decreasing of the extra oxygen may give two functions on the structure and carrier concentration of the CuO_2 planes. One is to introduce the charge-transfer between the carrier

reservoir (BiO–SrO) and conducting CuO_2 plane, as well as the change of modulation structure. By the study of the $(Bi, Pb)_2Sr_2(Ca, Y)Cu_2O_z$ system, Calestani *et al* [8] found that the double (Bi, Pb)O layer plays a competitive role (with respect to the CuO_2 plane) in accommodating the extra charge deriving from the substitution of Pb for Bi. The bottom of the Bi–O bands lies below the Fermi energy E_F, allowing a transfer of electrons to occur from the CuO_2 planes to the double BiO planes and creating doping holes on the Cu–O bands in this way [20, 21]. Because of the requirement of valence balance and the change of ionic radius, the Pb dopant causes the extra oxygen decrease resulting in the charge-transfer between the carrier reservoir (BiO–SrO) and the conducting CuO_2 plane. The carrier concentration decreases with increasing Pb content. Meanwhile, the incommensurate modulation structure is weakened as observed in this experiment. The other function is to increase the positive charge in BiO planes. It is important to point out here that the reduction of extra oxygen content in the Pb-doped Bi compounds is not entirely due to the difference in the valences between Pb^{2+} and Bi^{3+} as has been usually believed. The difference in the ionic sizes of Pb^{2+} and Bi^{3+} should make an important contribution to the reduction of the extra oxygen content as well. Because of the extra oxygen reduction caused by the different ionic sizes, the requirement of valence balance for Bi^{3+} may not be reached, resulting in the positive charge increasing in the BiO planes. By the attraction of the positive charge, the oxygen atoms located in CuO_2 planes shift to BiO planes and strengthen the distortion of CuO_2 planes as revealed in the Raman results. The Cu–O bond length increases, resulting in Cu valence change. In this way the carrier concentration of CuO_2 planes may be decreased. Meanwhile a net positive charge and hence the repulsion between the Bi_2O_2 layers increase, causing the increasing of *c*- and *b*-axes. The latter function of extra oxygen reduction can also be shown in annealing samples. After annealing in vacuum, further extra oxygen loss enhances the charge transfer. Meanwhile, the increasing of positive charge in BiO planes makes the shifting of oxygen atoms from the CuO_2 plane and the distortion of CuO_2 planes become bigger. This has been observed in the Raman results. The two functions work cooperatively and control the carrier concentration change. As a result, the carrier concentration changes from overdoped to underdoped with the reduction of extra oxygen. The distortion of CuO_2 planes becomes bigger and bigger, and an optimum distortion for the optimum superconductivity appears. For the same reason, all the samples reaches an optimum carrier concentration and an optimum T_{C0}.

The recent discovery of stripes in the underdoped cuprates [22] has brought renewed interest to the question of the existence of phase separation in the t–J and Hubbard models. Interest in this question began a decade ago, when evidence for phase separation in $La_2CuO_{4+\delta}$ was found [23]. There are, in fact, two main views regarding the origin of stripes. In the first, stripes form because of a competition between kinetic and exchange energies in doped antiferromagnets. The second approach starts with the assumption that without long-range Coulomb interactions, doped antiferromagnets phase separate. Stripe formation arises in this approach because the long-range Coulomb repulsion frustrates the phase separation, leading to an inhomogeneous charge density state [24]. In this experiment, the distribution of the charge in BiO planes caused by the reduction of extra oxygen is incommensurately modulated due to the incommensurate modulation structure. In fact, Zhu and Tafto have observed the charge modulation along the BiO double layer in the $Bi_2Sr_2CaCu_2O_{8+\delta}$ by electron microscope experiments [25]. We suggest that the charge-transfer between the carrier reservoir (BiO–SrO) and the conducting CuO_2 plane should be affected by the modulation structure existing in the $Bi_{1.6}Pb_{0.4}Sr_2CaCu_2O_\delta$ system. Both the charge-transfer and the CuO_2 plane distortion caused by the charge modulation distribution in BiO double planes should give an effect on the stripe formation.

Acknowledgment

This work was financially supported by the National Education Department of China.

References

[1] Cava R J 1990 *Science* **247** 656
[2] Tarascon J M *et al* 1988 *Phys. Rev.* B **38** 8885
[3] Shimakawa Y, Kubo Y, Manako T and Igarashi H 1989 *Phys. Rev.* B **40** 11 400
[4] Hentsch F, Winzek N, Mehring M, Mattausch Hj and Simon A 1989 *Physica* C **158** 137
[5] Distasio M, Müller K A and Pietronero L 1990 *Phys. Rev. Lett.* **64** 2827
[6] Dmowski W *et al* 1988 *Phys. Rev. Lett.* **61** 2608
[7] Pham A Q, Hervieu M, Maignan A, Michel C, Provost J and Raveau B 1992 *Physica* C **194** 243
[8] Calestani G, Francesconi M G, Salsi G, Andreetti G D and Migliori A 1992 *Physica* C **197** 283
[9] Anderson P W 1987 *Science* **235** 1196
[10] Groen W A *et al* 1989 *Solid State Commun.* **72** 697
[11] Gao Y, Pernambuco-Wise P, Crow J E, O'Reilly J, Spencer N, Chen H and Salomon R E 1992 *Phys. Rev.* B **45** 7436
[12] Chen X H, Ruan K Q, Qian G G, Li S Y, Cao L Z, Zou J and Xu C Y 1998 *Phys. Rev.* B **58** 5868
[13] Hinnen C, Nguyen van Huong C and Marcus P 1995 *J. Electron Spectrosc. Relat. Phenom.* **73** 293
[14] Iwai Y, Hoshi Y, Saito H and Takata M 1990 *Physica* C **170** 319
[15] Nagoshi M, Suzuki T, Fukuda Y, Terashima K, Nakanishi Y, Ogita M, Tokiwa A, Syono Y and Tachiki M 1991 *Phys. Rev.* B **43** 10 445
[16] Mao Z Q, Tian M L, Ji M R, Zhu J S, Zuo J, Wang R P, Wang Y and Zhang Y H 1994 *Phys. Rev.* B **49** 49
[17] Zandbergen H W, Groen W A, Mijhoff F C, Van Tendeloo G and Amelinckx S 1989 *Physica* C **156** 325
[18] Kakihana M, Osada M, Käll M, Börjesson L, Mazaki H, Yasuoka H, Yashima M and Yoshimura M 1996 *Phys. Rev.* B **53** 11 796
[19] Pantoja A E, Pooke D M, Trodahl H J and Irwin J C 1998 *Phys. Rev.* B **58** 5219
[20] Herman F, Kasowski R V and Hsu Y W 1988 *Phys. Rev.* B **38** 204
[21] Retoux R, Studer F, Michel C, Raveau B, Fontaine A and Dartyge E 1990 *Phys. Rev.* B **41** 193
[22] Tranquada J M, Axe J D, Ichikawa N, Moodenbaugh A R, Nakamura Y and Uchida S 1997 *Phys. Rev. Lett.* **78** 338
[23] Jorgensen J D *et al* 1988 *Phys. Rev.* B **38** 11 337
[24] Kivelson S A and Emery V J 1996 *Synth. Met.* **80** 151
[25] Zhu Y and Tafto J 1996 *Phys. Rev. Lett.* **76** 443